SURFACE HEAT BUDGETS AND SEA SURFACE TEMPERATURE IN THE PACIFIC WARM POOL DURING TOGA COARE

Shu-Hsien Chou*, Wenzhong Zhao, and Ming-Dah Chou
Laboratory for Atmospheres
NASA/Goddard Space Flight Center
Greenbelt, MD, USA

Abstract

The daily mean heat and momentum fluxes at the surface derived from the SSM/I and Japan's GMS radiance measurements are used to study the temporal and spatial variability of the surface energy budgets and their relationship to the sea surface temperature during the COARE intensive observing period (IOP). For the three time legs observed during the IOP, the retrieved surface fluxes compare reasonably well with those from the IMET buoy, RV Moana Wave, and RV Wecoma. The characteristics of surface heat and momentum fluxes are very different between the southern and northern warm pool. In the southern warm pool, the net surface heat flux is dominated by solar radiation which is, in turn, modulated by the two Madden-Julian oscillations. The surface winds are generally weak, leading to a shallow ocean mixed layer. The solar radiation penetrating through the bottom of the mixed layer is significant, and the change in the sea surface temperature during the IOP does not follow the net surface heat flux. In the northern warm pool, the northeasterly trade wind is strong and undergoes strong seasonal variation. The variation of the net surface heat flux is dominated by evaporation. The two westerly wind bursts associated with the Madden-Julian oscillations seem to have little effect on the net surface heat flux. The ocean mixed layer is deep, and the solar radiation penetrating through the bottom of the mixed layer is small. As opposed to the southern warm pool, the trend of the sea surface temperature in the northern warm pool during the IOP is in agreement with the variation of the net heat flux at the surface.

1. INTRODUCTION

A small variation of sea surface temperature (SST) associated with the eastward shift of the Pacific warm pool during the ENSO events affects the global climate. Thus, the Tropical Ocean Global Atmosphere (TOGA) Coupled Ocean-Atmosphere Response Experiment (COARE) was conducted with the aim to better understand various physical processes responsible for the SST variation (Webster and Lukas 1992). To understand and predict SST variations, accurate estimates of air-sea fluxes are essential. In this study, we validate the satellite-derived surface radiative (Chou et al. 1998) and turbulent fluxes (Chou et al. 1997) using those measured at the IMET buoy, RV Moana Wave and RV Wecoma during the TOGA COARE intensive observing period (IOP; Weller and Andersaon 1966).

*Corresponding author address: Shu-Hsien Chou, Laboratory for Atmospheres, Code 912, NASA/Goddard Space Flight Center, Greenbelt, MD 20771, USA; e-mail: chou@agnes.gsfc.nasa.gov.

The western equatorial Pacific is characterized by frequent heavy rainfall, large solar heating and weak mean winds with highly intermittent westerly wind bursts. Thus, the ocean mixed layer has been found to be generally very shallow with a barrier layer to stop the entrainment of cold waters from the deeper thermocline except for very strong westerly wind bursts (Lukas and Lindstrom 1991; Anderson et al. 1996). In addition, the horizontal advection of heat in the warm pool has been estimated to be very small due to small SST gradients and weak currents (Niiler and Stevenson 1982; Enfield 1986). In this paper, we use an ocean mixed-layer heat budget without entrainment to study the importance of the transmission of solar radiation to SST variations.

Two 40-50 days Madden Julian oscillations (MJOs) were observed to propagate eastward from the Indian Ocean to the Central Pacific during the IOP (Gutzler et al. 1994; Lin and Johnson 1996; Lau and Sui 1997; Sui et al. 1997). Two super cloud clusters and westerly wind bursts lasting for about 2-3 weeks were associated with the two MJOs. The super cloud

clusters reduce solar heating while the westerly wind bursts increase the evaporative cooling. In this study, we also investigate the impacts of the two MJOs on the surface heat budgets and the SST variation of the warm pool.

2. METHODOLOGY AND DATA

Chou et al. (1998) derived daily mean surface net solar and longwave fluxes from the radiances measured by the Japan's GMS for the western Pacific warm pool (defined as 10°S-10°N, 135°E-175°E hereafter) for the IOP, using the empirical relationships between the satellite-measured radiances and the surface downward radiative fluxes derived from several COARE radiation sites near the Intensive Flux Array (IFA). These sites do not include the IMET buoy, Moana Wave and Wecoma. Chou et al. (1997) used a stability-dependent bulk scheme to estimate daily surface turbulent fluxes from the surface winds and surface humidity retrieved from the radiances measured by the Special Sensor Microwave/Imager (SSM/I), NCEP SST, and sea-air temperature difference of the ECMWF. Daily surface radiative fluxes (with 1°x1° latitude-longitude resolution) computed by Chou et al. (1998) and the turbulent fluxes (with 2°x2.5° latitude-longitude resolution) calculated based on Chou et al. (1997) for the warm pool from 1 November 1992 to 28 February 1993 are used in this study. The turbulent fluxes are bilinearly interpolated to have one degree resolution.

3. RESULTS

The averaged satellite-retrieved surface fluxes at (1.5°S, 155.5°E) and (1.5°S, 156.5°E) are compared with those from the RV Moana Wave, RV Wecoma, and IMET buoy located in the IFA for three time legs observed during the IOP in Table 1. Leg 1 (14 November 1992 - 3 December 1992) was characterized by clear skies and large spatial scales of low winds within the IFA. Leg 2 (20 December 1992 - 11 January 1993) started with strong westerly wind bursts across the IFA and then shifted back to clear skies with fairly uniform light winds in January 1993. Leg 3 (27 January 1993 - 3 February 1993) was characterized by eastward propagating surges of westerlies and scattered clouds. There is significant variability among the three legs. The net surface heating for the ocean is positive during Leg 1, as a result of smaller cloudiness and low wind. On the other hand, the net heating is negative for the other two legs, due to reduced solar heating, and strong evaporative cooling associated with westerly wind bursts (Leg 2) and squalls (Leg 3). The retrieved fluxes agree reasonably well with those of the three surface platforms. In addition, daily values of the satellite-retrieved fluxes during the IOP are in good agreement with that of the IMET measurements (not shown).

Table 1. Time-mean surface fluxes derived from satellite measurements (Sat) and from surface observations at the RV Moana Wave (MW), RV Wecoma (Wec), and IMET buoy for three legs during COARE IOP. F_{SW}, F_{LW}, F_{SH}, F_{LH}, F_{net}, and τ denote net solar, net infrared, sensible heat, latent heat, net heat, and momentum fluxes at the surface, respectively. Units are W m^{-2} for heat fluxes, and 10^{-4} N m^{-2} for wind stress.

Flux	leg 1 (11/14-12/3/92)				leg 2 (12/20/92-1/11/93)				leg 3 (1/27-2/3/93)			
	Sat	MW	IMET	Wec	Sat	MW	IMET	Wec	Sat	MW	IMET	Wec
F_{SW}	231.0	224.7	227.8	223.1	175.6	162.0	162.3	168.2	182.9	164.0	180.3	192.8
F_{LW}	56.5	62.9	64.4	62.2	48.9	52.0	52.7	55.5	51.7	53.6	55.0	59.5
F_{SH}	5.0	6.0	6.8	4.6	6.2	8.4	10.0	9.1	7.4	9.4	8.3	13.9
F_{LH}	79.4	89.7	84.6	86.1	128.1	118.8	110.1	120.3	130.1	137.6	139.3	149.6
F_{net}	90.1	66.2	71.9	70.3	-7.7	-17.2	-10.5	-16.7	-6.3	-36.6	-22.4	-30.2
τ	198	205	183	174	537	638	653	636	542	535	546	567

The spatial distributions of surface net heat flux, F_{net}, rate of SST change, and penetration of solar radiation through bottom of the mixed layer, f(h) F_{sw}, averaged over the IOP are shown in Figs. 1a, 1b, and 1c, respectively. As expected, the ocean gains heat in the summer (southern) hemisphere while loses heat in the winter (northern) hemisphere, with the net heat flux ranging from -80 W m^{-2} in the northeastern section of the warm pool to 40 W m^{-2} north of New Guinea. Averaged over the warm pool, the net heating is only 0.7 W m^{-2}. This result is consistent with the studies of Godfrey and Lindstrom (1989) and Godfrey et al. (1991) that the mean surface net heat flux into the warm pool is small (<10 W m^{-2}). On the other hand, Fig. 1b shows that, except near the southern edge, the warm pool cools during the IOP. The cooling increases northward and reaches a maximum exceeding 0.5 °C $month^{-1}$. Averaged over the warm pool, the SST cools at a rate of 0.14 °C $month^{-1}$, which does not agree with a 0.7 W m^{-2} of net surface heat flux. This discrepancy is particularly large in the southern warm pool. For example, the surface net heat flux north of New Guinea has a maximum >40 W m^{-2}, but the SST cools at a rate of 0.3 °C $month^{-1}$. Figure 1c shows that this is mainly due to the fact that much of the solar flux incident at the surface penetrates through the bottom of the mixed layer and is not available for heating the layer.

It can be seen that the solar radiation lost through the bottom of the mixed layer is small (due to a deep mixed layer) in the northern warm pool but is large in the southern warm pool (due to a shallow mixed layer). The mean value is ~26 W m^{-2} for the former and ~45 W m^{-2} for the latter. Averaged over the warm pool and IOP, the loss of solar radiation is ~35 W m^{-2}, which is significantly larger than the surface net heat flux of 0.7 W m^{-2}. Thus, the cooling of SST in the warm pool during the IOP is primarily due to this loss of solar radiation, although the infrequent westerly wind bursts may deepen the mixed layer to the top of the thermocline and entrain cold water from below.

The impacts of the two MJOs on the surface heat budgets and SST evolutions have been studied. The time series of 5-day running means of SST, net surface solar flux, latent heat flux, mixed-layer depth, h, wind stress, and mixed-layer heat budgets averaged over the southern and northern warm pool, respectively are shown in Figs. 2 and 3. The characteristics of surface heat and momentum fluxes during the IOP are very different between the southern warm pool and the northern warm pool. In the southern warm pool, winds are generally weak except during short episodes of westerly wind bursts. As a result, the solar heating at the surface is much larger than the evaporative cooling. Averaged over the southern warm pool and the IOP, it is 196 W m^{-2} for the solar heating and only 108 W m^{-2} for the evaporative cooling, and the impact of the MJOs on the surface solar flux is significantly larger than the impact on the latent heat flux. The monthly variation of the net surface heat flux is dominated by the solar radiation. Associated with the weak surface winds, the ocean mixed layer in the southern warm pool is shallow with a mean depth of ~28 m. Because of the shallow mixed layer, a significant amount of solar radiation incident at the surface penetrates through the bottom of the mixed layer (~45 W m^{-2}), and the rate of change in the surface temperature does not follow the net surface heat flux.

In the northern warm pool, the northeasterly trade wind is strong with a maximum exceeding 8 m s^{-1} for the IOP-mean. The domain-averaged latent heat flux during the IOP is 148 W m^{-2}, which is much larger than the latent heat flux in the southern warm pool. The monthly variation of the net surface heat flux is dominated by the latent heat flux which is, in turn, dominated by the seasonal change in the strength of the northeasterly trade wind. Because of the strong surface wind, the mean mixed layer is deep, ~56 m, and the solar radiation penetrating through the bottom of the mixed layer is small. The rate of change in SST during the IOP follows closely the net surface heat flux, except for a short period of 11-21 January 1993. Also different from the southern warm pool, the MJOs does not have a clear impact on the surface heat budgets of the northern warm pool.

4. REFERENCES

Anderson, S. P., R. A. Weller, and R. B. Lukas, 1966: Surface buoyancy forcing and the mixed layer of the western Pacific warm pool: observations and 1D model results. *J. Climate*, 9, 3056-3085.

Chou, M.-D., W. Zhao and S.-H. Chou, 1998: Radiation budgets and cloud radiative forcing in the Pacific warm pool during TOGA COARE. *J. Geophys. Res.*, 103, 16967-16977.

Chou, S.-H., C.-L. Shie, R. M. Atlas and J. Ardizzone, 1997: Air-sea fluxes retrieved from Special Sensor Microwave Imager data. *J. Geophys. Res.*, 102, 12705-12726.

Enfield, D. B. 1986: Zonal and seasonal variations of the near-surface heat balance of the equatorial Pacific Ocean. *J. Phys. Oceanogr.*, 16, 1038-1054.

Godfrey, J. S., M. Nunez, E. F. Bradley, P. A. Coppin, and E. J. Lindstrom, 1991: On the net surface heat flux into the western equatorial Pacific. *J. Geophy. Res.* 96, 3343-3357.

Gutzler, D., G. N. Kiladis, G. A. Meehl, K. M. Weickman, and M. Wheeler, 1994: The global climate of December 1992-February 1993. Part II: Large-scale variability across the tropical western Pacific during TOGA COARE. *J. Climate*, 7, 1606-1622.

Lau, K.-M., C.-H. Sui, 1997: Mechanism of short-term sea surface temperature regulation: observations during TOGA COARE. *J. Climate*, 10, 465-472.

Lin, X., and R.H. Johnson, 1996: Kinematic and thermodynamic characteristics of the flow over the western Pacific warm pool during TOGA COARE. *J. Atmos Sci.*, 53, 695-715.

Lukas, R., and E. Lindstrom, 1991: The mixed layer of the western equatorial Pacific Ocean. *J. Geophy. Res.*, 96 (suppl.), 3343-3357.

Niiler, P., and J. Stevenson, 1982: The heat budget of tropical warm pools. *J. Mar. Res.*, 40 (suppl.), 465-480.

Sui, C.-H., X. Li, K.-M. Lau, and D. Adamac, 1997: Mutiscale air-sea interactions during TOGA COARE. *Mon. Wea. Rev.*, 125, 448-462.

Webster, P. J. and R. Lukas, 1992: TOGA COARE: The TOGA coupled ocean-atmosphere response experiment. *Bull. Amer. Meteor. Soc., 73,* 1377-1416.

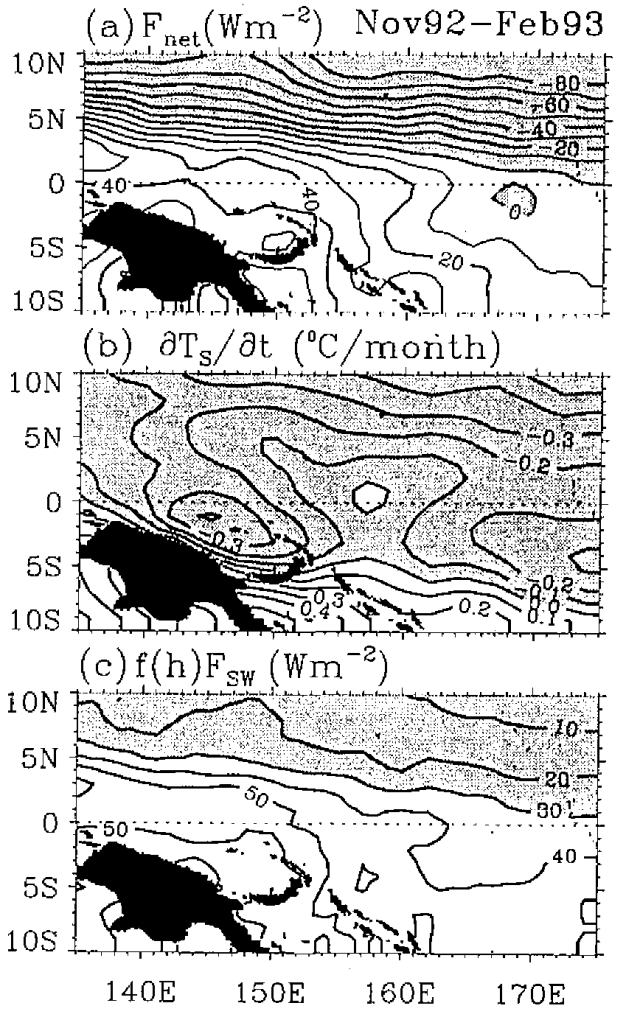

Fig. 1. Mean fields of (a) net surface heat flux, F_{net}, (b) rate of SST change, $\partial T_S/\partial t$, and (c) penetration of solar radiation at bottom of ocean mixed layer, f (h) F_{SW}, for COARE IOP.

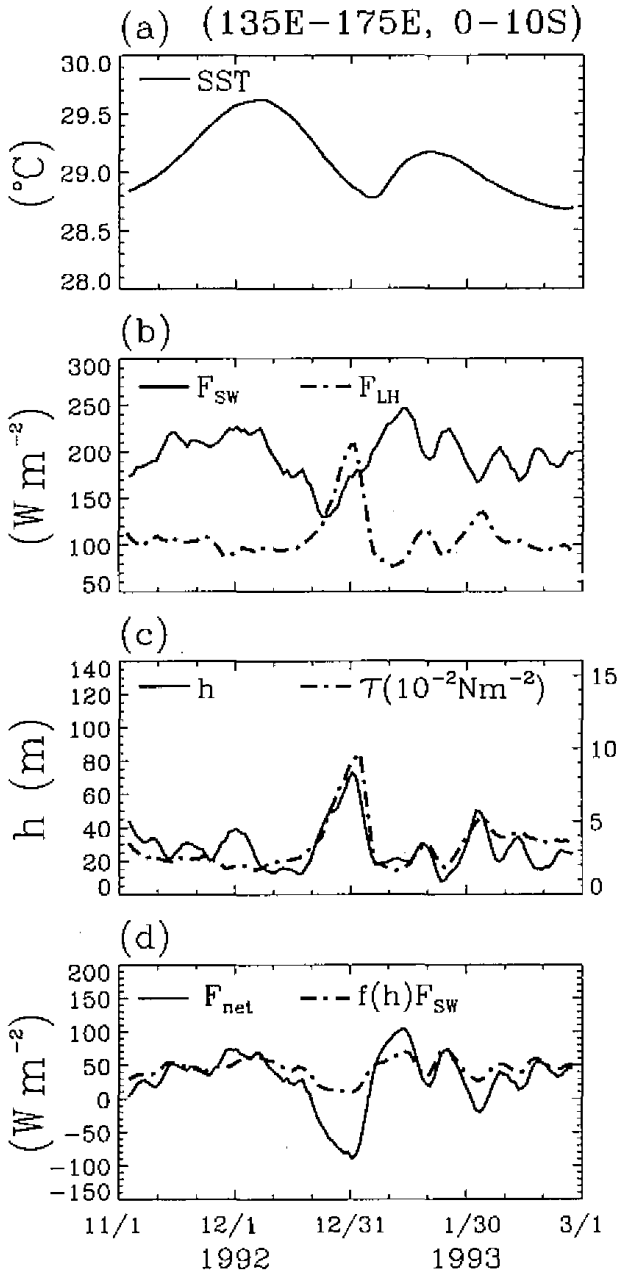

Fig. 2. Time series of 5-day running mean (a) SST, (b) net solar flux, F_{sw}, and latent heat flux, F_{LH}, (c) mixed-layer depth, h, and scalar averaged wind stress, τ, and (d) net surface heat flux, F_{net}, and penetration of solar radiation through bottom of mixed layer, f(h) F_{sw}, averaged over the region 0-10°S and 135°E-175°E during COARE IOP.

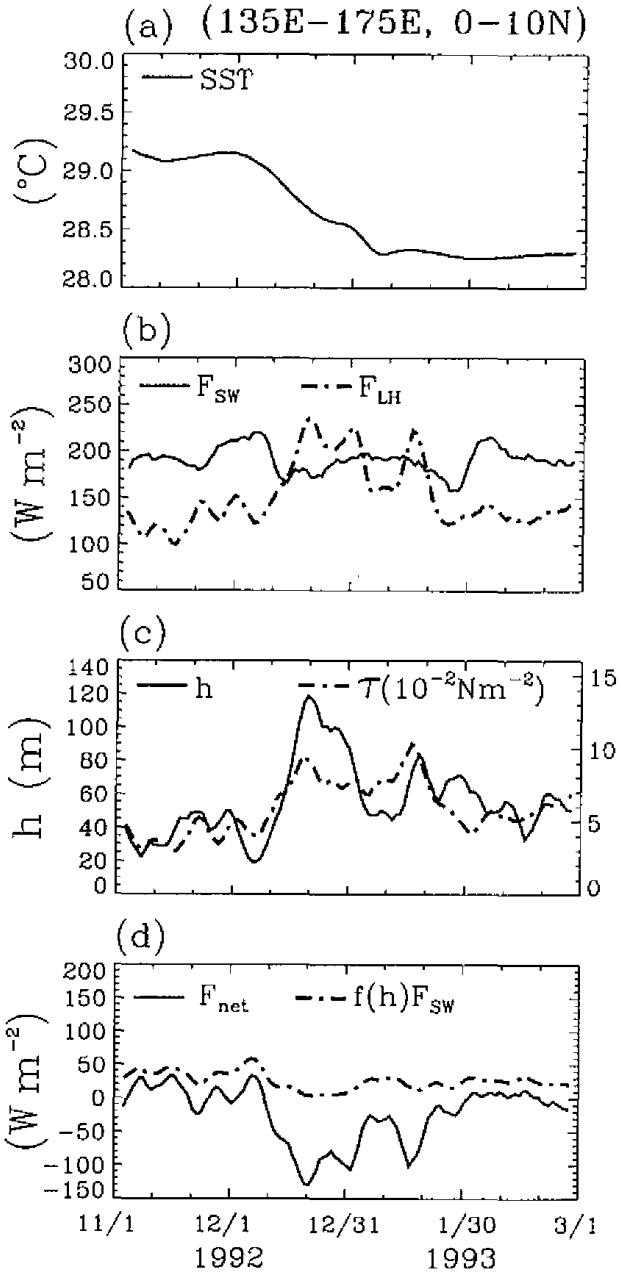

Fig. 3. Time series of 5-day running mean (a) SST, (b) net solar flux, F_{sw}, and latent heat flux, F_{LH}, (c) mixed-layer depth, h, and scalar averaged wind stress, τ, and (d) net surface heat flux, F_{net}, and penetration of solar radiation through bottom of mixed layer, f(h) F_{sw}, averaged over the region 0-10°N and 135°E-175°E during COARE IOP